VII. MIXED DIMERS

VII.1. INTRODUCTION

Continuing our investigation of dimer production (ref.1) we have tried to detect mixed dimers in nozzle beams of mixtures; NeAr and HeNe dimers were observed with sufficient intensity to determine the total collision cross section. A similar attempt for H_2Ar was partially hampered by the circumstance that the corresponding HAr^+ ion must be detected on the wing of the thousand times larger Ar^+ peak. Our search for H_2He, H_2Ne and HeAr dimers was not successful, due to masking ion peaks, H_5^+ for HHe^+, $^{21}Ne^+$ for $H^{20}Ne^+$, and CO_2^+ for $HeAr^+$.

For the Ne-Ar mixture (3 Ne :1 Ar in the source) we observe an optimum $NeAr^+$ signal of about 0.1% of the Ar^+signal with a signal to noise ratio S/N = 30, at a time constant τ = 1 sec. A similar result is obtained for the He-Ne mixture. At the moment these optimum signals seem too small for electric beam resonance measurements, which appear interesting in view of recent discussions of the electric dipole moment of these mixed inert gas dimers (ref. 2).

The existence of an H_2He dimer is questionable (ref. 3). The situation can be compared to that of the He dimer. Our results do not throw new light on this problem.

A positive aspect of the mixed clusters and their mass spectrometric detection is the low probability for fragmentation of larger clusters to the mixed dimer ion. For instance, using the Ne-Ar mixture, signals of Ar_3^+– and Ar_4^+–ions are found, but no signals of $NeAr_2^+$-ions. Even conceding that neutral $NeAr_2$ is present in the beam, $NeAr^+$ will be formed as fragment ion with smaller probability than Ar_2^+. In complete agreement herewith we observe a constant collision cross section for the $NeAr^+$ parent up to pressures substantially higher than those at which the Ar_2– Ar_2^+ correspondence breaks down, i.e. P_L (sect. VII.3); at these high pressures the $NeAr^+$ signal goes through a maximum. For $HeNe^+$ a constant collision cross section is observed up to pressures where the $HeNe^+$ signal has dropped already to .3 of its maximum value.

As will be shown in sect. VII.4 the observed mixed dimer intensities can be fairly well predicted from a source equilibrium calculation.

Concerning the production of pure dimers from gas mixtures, e.g. Ar_2 from the Ne-Ar mixture, we observe a significant increase through the presence of the lighter gas compared to the dimer intensity from pure gases, at the same partial pressure and temperature in the source. This increase points definitively in the direction of dimer formation downstream the nozzle, where, due to the extra acceleration of the beam molecules by the light carrier gas, the formation temperature T_f is lower than for pure gas jets, see sect. VII.4. Similar observations have been reported in ref. 4.

In fig. VII.1.2a and 2b the intensities are displayed for the mixed gases as a function of the source pressure P_0. The mixtures have been prepared by us from commercial pure gases; we have used 1:3 mixtures of Ar in Ne, Ne in He and Ar in H_2.

The monomer signals nearly coincide for Ne-Ar and He-Ne mixtures.

When the difference in detection efficiency is taken into account (see appendix A 2) we find no enhancement of the heavier monomer in the beam. On the other hand, for the H_2-Ar mixture with its large mass difference between the components, an order of magnitude less H_2 is measured with respect to Ar. This cannot be explained by a difference in detection efficiency. The light carrier gas is lost from the central beam by collisions with the heavier component (ref. 4). As soon as the Ar_2 signal appears, the H_2 monomer signal becomes practically independent of P_0, presumably due to increasing losses caused by the Ar dimer formation process. Energy is liberated in the dimer formation process; corresponding linear momentum is mainly imparted to the lighter component of the mixture.

For a pure Ar monomer beam a signal from Ar^{++} ions is observed, of about 10% of the Ar^+ signal, at an electron bombardment energy of 130 eV. In fig. VII. 1 the intensity of Ne^+ is corrected for this Ar^{++} signal (about 10% decrease).

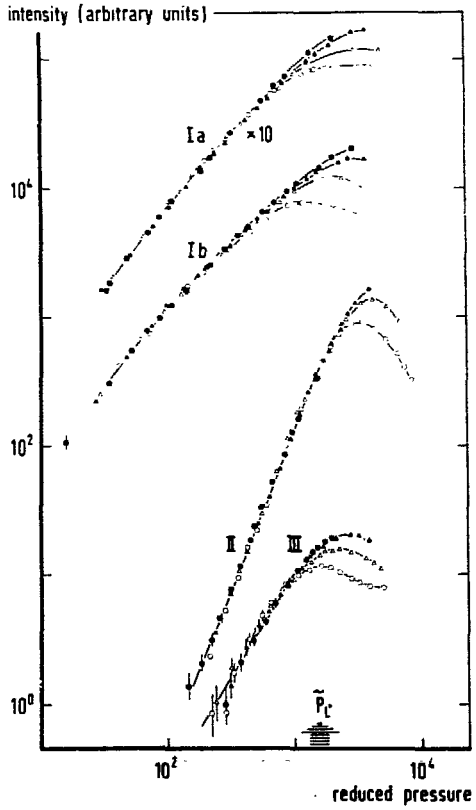

Fig. VII.1. Intensity vs. reduced pressure for Ne-Ar.
The Ne^+ intensity (Ia,displayed multiplied by a factor 10) nearly coincides with the Ar^+ intensity (Ib). Both monomer intensities are proportional to $P_0^{\alpha_1}$ at low pressures, with $\alpha_1 = 1.0 \pm .1$. For the Ar_2^+ (II) and $NeAr^+$ (III) intensity similar proportionalities hold with exponents $\alpha_2 = 2.5 \pm .2$ and $\alpha_3 = 1.6 \pm .2$, respectively. The intensities are measured at different source temperatures, $T_0 = 296$ K (●), $T_0 = 190$ K (▲), $T_0 = 148$ K (△), and $T_0 = 108$ K (O). The abscissa gives the true pressure in torr for $T_0 = 190$ K. At other temperatures reduction factors P_0/P_{red} are applied for each ion mass (table VII.1.) The shaded area indicates the reduced pressure $\tilde{P}_L$ at which the Ar_2 signal becomes contaminated by fragments of larger clusters.

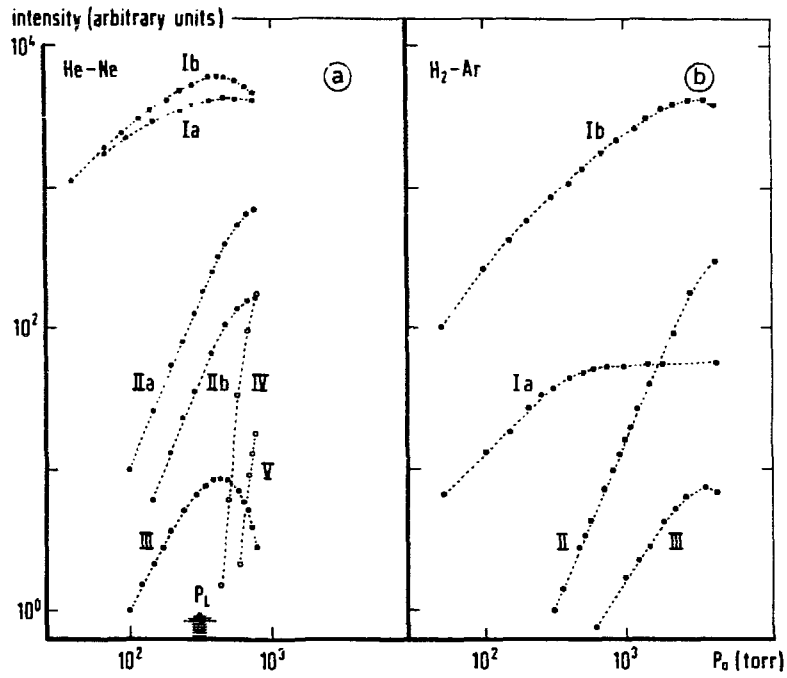

Fig.VII.2. Intensity vs. source pressure for He-Ne (a) and H_2-Ar (b).
For He-Ne (at source temperature T_0 = 31 K) the intensities are shown of the ions He^+ (Ia), $^{20}Ne^+$ (Ib), $^{20}Ne_2^+$ (IIa), $^{20}Ne^{22}Ne^+$ (IIb); at low pressures the ion signals are proportional to $P_0^{\alpha_m}$, with α_m = 1 (I), $\alpha_2 = 2.3 \pm .2$ and $\alpha_3 = 1.5 \pm .2$ (III). Also shown are the intensities for Ne_3^+ (IV) and Ne_4^+ (V). At the pressure $\tilde{P}_L$ fragment ions of larger clusters start to contribute to the Ne_2^+ signal. For H_2-Ar at source temperature T_0 = 173 K, the intensities are shown of H_2^+ (Ia), Ar^+ (Ib), Ar_2^+ (II), and HAr^+ (III). At low pressures the ion signals rise proportionally to $P_0^{\alpha_m}$, with $\alpha_{1a} = 1. \pm .2$, $\alpha_{1b} = 1. \pm .1$, α_2 = 2.3 ±.1, and α_3 = 1.5 ± .2, respectively.

In fig. VII.1 the pressure scale is the true one for T_0 = 190 K; for other temperatures the pressure scale is reduced for each ion signal by the factors P_0/P_{red}, given in table VII.1.

The $^{20}Ne\,^{40}Ar^+$ ion signal could be contaminated by Ar_3^{++} ions, possessing the same e/m ratio. However, for a pure Ar beam no Ar_3^{++} has been found; therefore we exclude this possibility.

We have not found signals of $^{22}Ne^{40}Ar^+$ or $^4He^{22}Ne^+$ ions; their intensity can be estimated to be an order of magnitude lower than that observed for $^{20}Ne^{40}Ar^+$ and $^4He^{20}Ne^+$ ions; this is beneath our detection limit.

Our mass spectrometer has a limited suppression of neighbouring mass peaks; for a pure Ar beam about .03% of the Ar^+ signal is measured at the mass-setting for HAr^+. The mixed dimer signal in the case of H_2-Ar, HAr^+, must be detected on the wing of a thousand times larger $^{40}Ar^+$ monomer peak. Therefore, the intensities of fig.VII.2b should be taken with some reserve. However, the scattering results of the next section prove that a mixed dimer signal is present. No attempt with a D_2-Ar mixture has been made yet.

The partial pressure for Ar at P_L is roughly equal to $\frac{1}{2}P_L$ found for pure Ar (cf. ch. III), in accordance with ref.4.

In fig. VII.4a and 4b the cross section for the He-Ne and the H_2-Ar mixture are given each for one source temperature (T_0 = 31 K and T_0 = 90 K, respectively), and one scattering partner (He and Kr, respectively). Here too, the cross sections displayed are corrected for the finite angular resolution. For the He^+, Ne^+, and $HeNe^+$ signal the cross sections are again independent of P_0. From the constant behaviour of σ_{HeNe} we infer that no larger mixed clusters, if present at all, contribute to the $HeNe^+$ signal. One obtaines $\sigma_{HeNe} = (1.83 \pm .06).\frac{1}{2}(\sigma_{Ne} + \sigma_{He})$ with He as scattering partner.

At $P_0 < 300$ torr the Ne_2 cross section is measured, yielding $\sigma_{Ne_2} / \sigma_{Ne} = 1.75 \pm .06$. Here, the partial Ne pressure at P_L = 300 torr is about equal to P_L in the pure Ne case of ch. IV. For $P_0 > P_L$ the dimer ion cross section rises to values near to those of the cross section for the larger cluster ions, Ne_3^+ and Ne_4^+.

In order to obtain larger mixed dimer signals and to reduce the influence of the limited mass separation (see sect. VII.2) we have used a different source temperature and gas mixture in the measurement of the cross sections of H_2-Ar (T_0 = 90 K vs. T_0 = 173 K used for the intensities in fig. VII.2b, and a 8:1 mixture vs. 3:1). As in fig. VII.2b the H_2^+ ion signal assumes a nearly constant value over the pressure range where dimer signals are present; this constant signal is about 10% of the Ar^+ signal (vs. 1.5-3% in fig. VII.2b). At a source

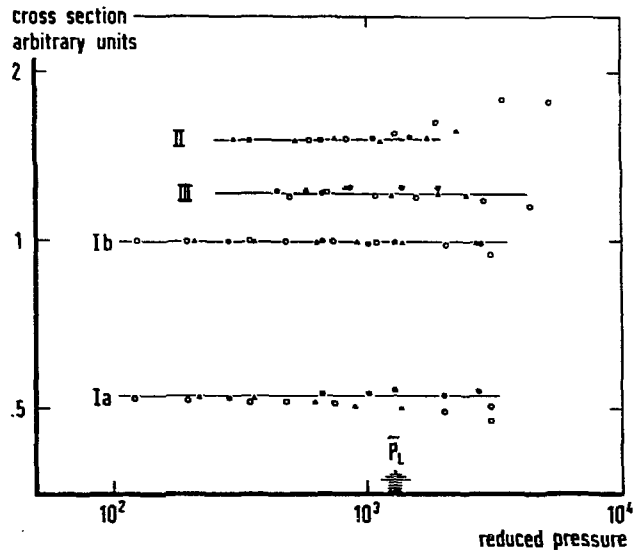

caption to fig. VII.3

Fig. VII.3. Apparent cross section vs. reduced pressure for the Ne-Ar mixture with He as scattergas. The cross sections are diplayed relative to the Ar monomer cross section; they are measured at source temperatures T_0 = 296 K (▲), T_0 = 210 K (●), and T_0 = 120 K (O); for the reduction of the pressure scale interpolated P_0/P_{red} values are used, see table VII.1. From $P_{red} < \tilde{P}_L$ the Ar_2 cross section is obtained. For NeAr the results are independent of pressure over the whole pressure range.

Dimers of the heavier component in the mixture are detected. In contrast to the case of pure gases, their intensity is proportional to $P_0^{\alpha_2}$, with α_2 larger than 2 (see caption of fig. VII. 1 and 2); for pure gases $\alpha_2 = 2$ has been found (ref. 1, ch. III and IV). At the same source temperature and partial source pressure the dimer intensity from the mixture has increased with respect to that of the pure gas. For a discussion see sect. VII.4.

The monomer intensities are about proportional to P_0 at low pressures; the mixed dimer signals have pressure exponents α_3 smaller than 2. The exact values are given in the captions.

TABLE VII.I

		T_0 (K)						β_i
		108	148	190	296	120	210	
Ne^+, Ar^+	(I)	.65 ± .1	.8 ± .1	1	1.5±.1	.7	1.1	.85 ± .1
Ar_2^+	(II)	.35 ± .02	.55 ± .03	1	2.1±.1	.4	1.4	2.1 ± .1
$NeAr^+$	(III)	.47 ± .05	.65 ± .07	1	1.6±.1	.5	1.2	1.6 ± .1

Table VII. 1 Reduction factors $f = P_0 / P_{red}$ for Ne-Ar
The values for f at $T_0 = 120$ K and $T_0 = 210$ K have been interpolated, using the approximation $f \propto T_0^{\beta_i}$. The values for β_i are given in the last column.

VII.3 SCATTERING

In fig. VII.3 the total collision cross sections vs. reduced source pressure are displayed relative to the Ar monomer cross section, for the different ion signals of the Ne-Ar mixture; He was used as scattering partner. The cross sections at three different source temperatures T_0 = 120, 210 and 296 K are collected in one figure by a similar reduction of the pressure scale as for the intensities; for T_0 = 120 and 210 K interpolated reduction factors are used, see table VII.1. The experimental cross sections are corrected for the finite angular resolution following ref. 5.

At low pressures all cross sections are independent of P_0, indicating a direct correspondence between ions and neutrals.

The ratio of the cross section $\sigma_{Ar_2}/\sigma_{Ar}$ is found to be 1.52± .02, with He as target molecule. The cross section of the mixed dimer σ_{NeAr}, is seen to be (1.61 ± .02) times $\frac{1}{2}(\sigma_{Ar} + \sigma_{Ne})$.

With Ar as scattering partner we find for $\sigma_{Ar_2}/\sigma_{Ar} = 1.36 \pm .02$ and $\sigma_{NeAr} = (1.45 \pm .02).\ \frac{1}{2}(\sigma_{Ar} + \sigma_{Ne})$ at a source temperature T_0 = 210 K.

For the Ar_2^+ signal a source pressure $\tilde{P}_L$ can be defined in fig. VII.3; at $\tilde{P}_L$ the cross section starts to rise above its constant low pressure value. The pressure P_L is 500 torr for T_0 = 120 K, 1800 torr for T_0 = 210 K; for T_0 = 294 K no rise of the Ar_2^+ cross section is yet observed, i.e. $P_L > 4000$ torr. Indicated in fig. VII.1 and 3 is $\tilde{P}_L$, obtained from the aforementioned P_L values and the reduction factors of table VII.1 for the Ar_2^+ signal.

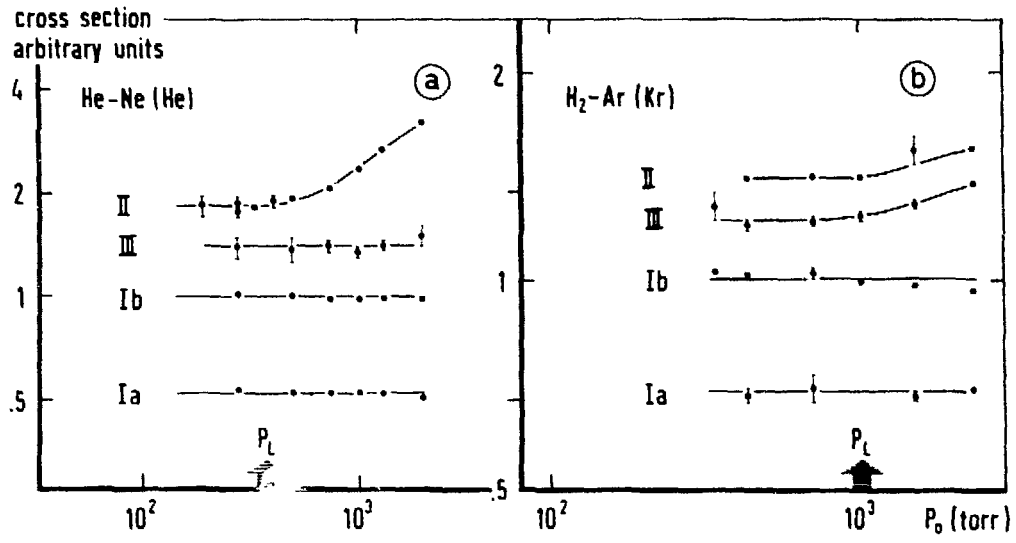

Fig. VII.4 Apparent cross section vs. source pressure P_0, (a) for a 3:1 He-Ne and (b) for a 8:1 H_2-Ar mixture with He and Kr as target gas, at temperatures T_0 = 31 K and 90 K, respectively. In the left part the He^+ (Ia), Ne^+ (Ib), and $HeNe^+$ (III) attenuations correspond for all pressures, those for Ne_2^+ (II) only for $P_0 < P_L$, to cross sections of well defined neutral particles.
In the right part the attenuations of H_2^+ (Ia), Ar^+ (Ib), Ar_2^+ (II) and HAr^+ (III) correspond each to a unique neutral parent for $P_0 < P_L = 10^1$ torr. At pressure $P_0 > P_L$ larger clusters contribute to both dimer signals.

pressure P_0 = 1000 torr both the Ar^+ and the HAr^+ ion signal go through a maximum; the maximum Ar_2 and HAr signal are 10% and 2% of the Ar^+ signal, respectively. The signal to noise ratio of the HAr^+ ion signal here, is 50, at a time constant of 1 sec.

From fig. VII.4b one infers a constant cross section for all ion signals at source pressures $P_0 < 1000$ torr. One obtaines $\sigma_{Ar_2}/\sigma_{Ar} = 1.35 \pm .02$ and $\sigma_{H_2Ar} = (1.45 \pm .02).\frac{1}{2}(\sigma_{H_2} + \sigma_{Ar})$. Due to the contribution of the Ar^+ signal to the HAr^+ signal as explained in the introduction, we present the cross section of the H_2Ar dimer as a lower limit; the value is estimated to be too low by 2% at maximum.

At $P_0 > 1000$ torr the cross section for the Ar_2^+ and the HAr^+ signal starts to rise, due to the admixture of larger clusters. For Ar_2^+ this rise has been observed earlier (ref. 1a); for HAr^+ this rise is the only indication in our investigation to the existence of larger mixed clusters. At the same pressures, signals of H_3^+ ions are detected too.

The decrease of the monomer cross section for Ar has been dealt with in an earlier paper (ref. 1a).

For a comparison of the observed mixed dimer concentration of NeAr and the equilibrium concentration in the source we calculated the partition function Z_{mix} ; the vibrational energy have been calculated by us in the J.W.K.B. approximation, using ε and R_m values for the Lennard-Jones 12-6 potential from ref. 6, see appendix A1. The rotational constant B has been taken at the equilibrium position of the two atoms, for all 5 vibrational levels. The resulting partition function is estimated to give values 40% too small. The estimate is based on similar Ar_2 results (sect. VI.2). From the partition functions the equilibrium constant $K_0 = n_{NeAr} / n_{Ne} \cdot n_{Ar}$ is calculated as a function of the source temperature T_0.

The experimental intensity ratio I_{NeAr} / I_{Ar} is divided by 1.25 to compensate for the increased detection efficiency, and by the calculated neon density in the source, to obtain values for K_{obs} . For a fixed source temperature T_0 the intensity ratios are used only for pressures lower than P_0, where the intensities reach their maxima (onset region). The resulting K_{obs} values are independent of the source pressure P_0 to within 10%. Therefore in fig. VII.7 only one point is given for each T_0. We find $K_{obs} \simeq K_0$.

Similarly, we compared the Ar_2 concentration with the data for pure Ar

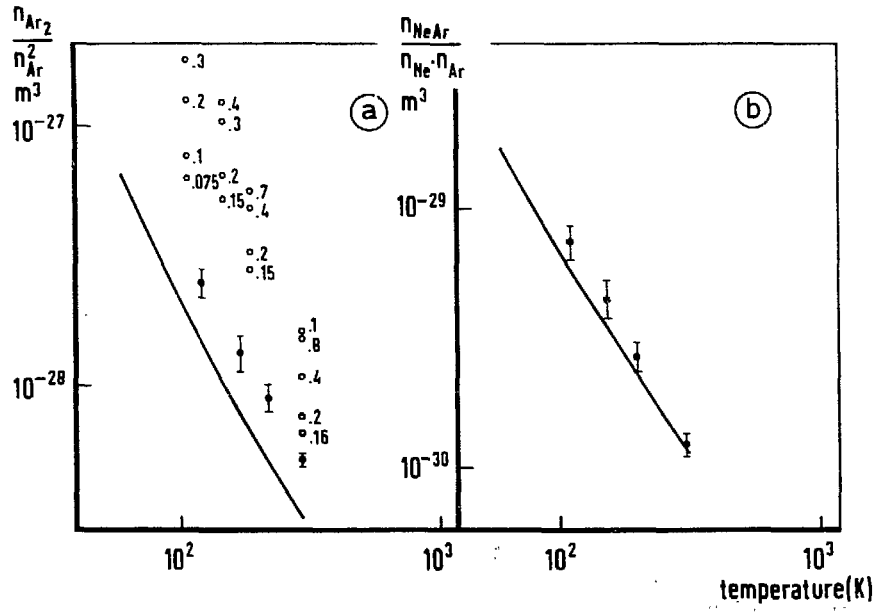

caption to fig. VII.5

Fig. VII.5 Equilibrium constant vs. temperature.

In the left part (a) the calculated curve K_0 is taken from sect. VI.2; the dots indicate the values for K_{obs} for Ar_2 from pure Ar (see fig. VI.2). The open circles indicate the values for K_{obs} for Ar_2 from the Ne-Ar mixture; n_1 stands for the partial Ar density in the source (in amagat). In the right part the dots correspond to the values of K_{obs} for NeAr, which are in good agreement with K_0 (solid line).

from sect. VI.2, for pressures lower than P_L (see sect. VII.3). In the onset region the Ar_2^+ intensity is proportional to $P_0^{2.5}$; consequently, the values for K_{obs} are pressure dependent. In fig. VII.7 we give the values at different pressures, as indicated in the caption.

With respect to sect. VI.2 an increase of the experimental dimer concentration is found, which amounts to a factor 4, at maximum. Thus, K_{obs} is pressure dependent and 4 to 8 times larger than $K_0 = n_{Ar_2}/n_{Ar}^2$. Both effects are attributed to an extra cooling during expansion due to the presence of the lighter Ne. They indicate strongly that the dimers observed are produced during the expansion.

The fact that $K_{obs} \simeq K_0$ for NeAr, while large discrepancies occur for Ar_2 from the Ne-Ar gas mixture, can be explained as follows; the NeAr dimer fraction is rather independent of the temperature T_f, whereas for Ar_2, with its two times larger potential minimum ε, this temperature T_f forms a very critical parameter. As discussed in sect. VI.4, the dimers are assumed to be formed downstream the nozzle at an effective equilibrium temperature $T_f < T_0$. Then $K_{obs} = K_f$, with

$$K_f = K_0 \cdot G(kT_f/\varepsilon)/G(kT_0/\varepsilon)$$

(sect. VI.4), where

$$G(x) = 1 + .254/x + .057/x^2 + .0107/x^3$$

is a function weakly dependent on x for $x \geq .5$.

For Ar_2 with it large ε-value the condition $x \geq .5$ is not fulfilled.

For the other mixed dimer H_2Ar and HeNe the results in general are similar and give no new insights; they do not yet justify an extensive calculation.

REFERENCES CHAPTER VII

1. a/A.v. Deursen, A. v. Lumig and J. Reuss, Int. J. Mass Spectrom. Ion Phys., *18* (1975) 129, chapter III of this thesis.
   b/ to be published, chapter IV of this thesis
2. R. L. Matcha and R. K. Nesbet, Phys. Rev., *160* (1967) 72.
   H. B. Levine, Phys. Rev., *160* (1967) 159
3. R. Gengenbach and Ch. Hahn, Chem Phys., L *15* (1972) 604
4. E. W. Becker, R. Klingelhöfer, and P. Lohse, Z. Naturforsch., A *17* (1962) 432
5. F. v. Busch, Z. Physik, *193* (1966) 412
6. B. N. Srivastava and K. P. Srivastava, J. Chem. Phys., *30* (1969) 984